water

MDPI

Opinion

Predicting the Hydraulic Conductivity of Metallic Iron Filters: Modeling Gone Astray

Chicgoua Noubactep [1,2,3]

[1] Department of Applied Geology, Universität Göttingen, Goldschmidtstraße 3, Göttingen D-37077, Germany; cnoubac@gwdg.de; Tel.: +49-551-393-3191
[2] Comité Afro-européen, Avenue Léopold II, Namur 41-5000, Belgium
[3] Kultur und Nachhaltige Entwicklung CDD e.V., Postfach 1502, Göttingen D-37005, Germany

Academic Editor: Miklas Scholz
Received: 28 January 2016; Accepted: 13 April 2016; Published: 20 April 2016

Abstract: Since its introduction about 25 years ago, metallic iron (Fe^0) has shown its potential as the key component of reactive filtration systems for contaminant removal in polluted waters. Technical applications of such systems can be enhanced by numerical simulation of a filter design to improve, e.g., the service time or the minimum permeability of a prospected system to warrant the required output water quality. This communication discusses the relevant input quantities into such a simulation model, illustrates the possible simplifications and identifies the lack of relevant thermodynamic and kinetic data. As a result, necessary steps are outlined that may improve the numerical simulation and, consequently, the technical design of Fe^0 filters. Following a general overview on the key reactions in a Fe^0 system, the importance of iron corrosion kinetics is illustrated. Iron corrosion kinetics, expressed as a rate constant k_{iron}, determines both the removal rate of contaminants and the average permeability loss of the filter system. While the relevance of a reasonable estimate of k_{iron} is thus obvious, information is scarce. As a conclusion, systematic experiments for the determination of k_{iron} values are suggested to improve the database of this key input parameter to Fe^0 filters.

Keywords: corrosion rate; numerical simulations; permeability loss; water treatment; zero-valent iron

1. Introduction

Due to their low-cost components, metallic iron-based filtration systems (Fe^0 filters) have a broad range of applications from small-sized units for the production of safe drinking water in remote and/or low-income communities (e.g., Africa, Latin America and South-East Asia) to large-scale reactive walls for groundwater remediation, progress in numerical simulation of such systems may reasonably be expected to increase the application potential of this proven environmentally-friendly technology.

Predicting the service life of Fe^0 filters is a fundamental aspect in discussing the suitability of this technology, both in terms of affordability and (long-term) efficiency [1–4]. The present state of the art has been shown to by unsatisfactory [3,5–12]. This situation is caused by several reasons. One reason is a misinterpretation of the essential reaction causing contaminant removal. A reduction reaction implying electrons transfer from Fe^0 to the contaminants (e.g., RCl = chlorinated hydrocarbon, *cf.* Equation (1)) can be at best a side reaction under environmental conditions [13–19].

$$Fe^0 + RCl + H^+ \Rightarrow Fe^{2+} + RH + Cl^- \quad (1)$$

Iron corrosion by water (*cf.* Equation (2)) is spontaneous and quantitative.

$$Fe^0 + 2H^+ \Rightarrow Fe^{2+} + H_2 \quad (2)$$

Iron corrosion is well-known as a major nuisance reaction in the present iron-based world causing billions of Euro of damage per year [20]. This reaction is quantitative even in situations where water is present as moisture only [21]. It is therefore clear that iron corrosion by water has to be considered as a major reaction in a context (water treatment or Fe^0/H_2O system) where water is the solvent ($[H_2O]$ = ~55.5 mol L^{-1}). Even if more powerful oxidizing agents (e.g., Cr^{VI}, Cu^{2+}, NO_3^-, O_2, RCl) should be present as solutes (even at the mg L^{-1} level), Equation (2) still needs to be considered a dominant reaction in Fe^0/H_2O systems.

It has been unambiguously demonstrated that contaminant reduction in Fe^0/H_2O systems is mediated by (i) Fe^{II} species (Equation (3)) and H_2 (Equation (4)), which are primary corrosion products and (ii) secondary and tertiary corrosion products, including Fe_3O_4 and green rusts [10,11,22–26].

$$2\,Fe^{2+} + RCl + H^+ \Rightarrow Fe^{3+} + RH + Cl^- \quad (3)$$

$$H_2 + RCl \Rightarrow RH + HCl \quad (4)$$

The fact that the Fe^0 surface is constantly shielded by a multi-layered oxide scale (see [11] and the references cited therein) implies that, even under oxic conditions (O_2 is available), Fe^0 oxidizes according to Equation (2). This reaction is even accelerated if reaction products (e.g., Fe^{II} species) are consumed (Le Chatelier's principle). Further details about this aspect of the iron corrosion process are summarized in [21].

The presentation above clearly shows that rate constants for modeling contaminant reductive transformations in Fe^0/H_2O systems should be exclusively based on Equations (3) and (4). Alternative strategies have been discussed in [16,19,27–30]. These alternative strategies are based on Equation (1) and mentioned herein for the sake of completeness.

Electrochemical reduction alone (Equation (1)) cannot explain all reported observations as (i) the generation of iron hydroxides and oxides for As or U removal [31,32] or (ii) the porosity loss of Fe^0 beds flushed with distilled water [33,34]. These obvious discrepancies between various modeling approaches for Fe^0 filters, however, had been a motivation for the discussion herein.

The following four facts suggest that it may be sufficient to characterize the long-term behavior of Fe^0 corrosion while considering the coupled removal efficiency of selected species added as contaminants to have a realistic picture of Fe^0 filters [10,11,25]: (i) Fe^0 corrosion by water is quantitative; (ii) contaminants are chemically reduced by some iron corrosion products; (iii) contaminants are present in trace amounts; and (iv) contaminants without redox properties are quantitatively removed. Thus, the most important parameter to design a Fe^0 filter is the long-term corrosion rate (k_{iron}; *cf.* Section 2) of the material to be used.

The aim of the present communication is to demonstrate that no reliable model for Fe^0 filters can be presented without relevant k_{iron} values. Domga *et al.* [35] recently summarized the results of mathematical modeling of the spatial description of the process of permeability loss in Fe^0 filters. Herein, it is shown that related temporal changes depend on k_{iron} values that are yet to be determined. The significance of k_{iron} will be first presented, followed by the specificity of Fe^0 materials as used in water treatment and environmental remediation.

2. The Rate Constant of Iron Corrosion (k_{iron} Value)

2.1. Descriptive Aspects

Kinetic studies on contaminant reductive transformation in Fe^0/H_2O systems currently use relationships like the following based on reactions similar to Equation (5):

$$\frac{d[RCl]}{dt} = -k \times [RCl] \times [H^+] \quad (5)$$

Following this approach, k values for individual contaminants (e.g., k_{RCl}) have been determined and partly tabulated for modeling purposes [16]; however, considering that Equation (1) is faulty as Equations (3) and (4) are the main sources of electrons for any contaminant in a Fe^0/H_2O system (indirect reduction). Accordingly, properly modeling the kinetics of any reductive transformation in Fe^0/H_2O systems depends on the accurate characterization of the kinetics of the production of Fe^{2+} and H_2 or the determination of the kinetics of Fe^0 corrosion by water (Equation (6)). The relationship defining k_{iron} can be written as:

$$\frac{d\left(Fe^0\right)}{dt} = -k_{iron} \times [H^+]^2 \quad (6)$$

where k_{iron} is the rate of iron corrosion and $[H^+]$ the concentration of protons. Reardon [36,37] has positively correlated k_{iron} and the volume of H_2 generated in the Fe^0/H_2O system. However, properly correlating both values depends on the description of individual systems and the characterization of possible H_2 sinks [38]. In other words, characterizing the kinetics of iron corrosion (at pH > 4.0) by determining the volume of generated H_2 is just an approximation. This approach is arguably nearer to reality than any reasoning based on Equation (5) [39].

The abundant literature on aqueous iron corrosion reveals that there are three basic kinetics laws that characterize the oxidation rates of Fe^0: (i) the parabolic rate law; (ii) the logarithmic rate law; and (iii) the linear rate law. These laws are modeled respectively as follows [40,41]:

$$x^2 = Kp \times t + x_0 \quad (7)$$

$$x = Kp \times \log(c \times t + b) \quad (8)$$

$$x = K_L \times t \quad (9)$$

where x is the thickness of the oxide scale on Fe^0; Kp is the parabolic rate constant for scale growth; K_L is the linear rate constant for scale growth; t is time; a and c are constants. As a rule, the x values (scale thickness) are correlated to the Fe^0 weight loss (metal loss) without considering the presence of individual corrosive species (e.g., Cl^-, CO_2, H_2O, H_2S, O_2). The parabolic rate law assumes that the concentrations of diffusing species at the oxide/metal and oxide/water interfaces are constant and that the oxide scale is uniform, continuous and of the single phase type [41]. This law is applicable to high temperature engineering problems and is recalled here only for the sake of completeness. The logarithmic and the linear rate laws are more likely to be applicable to Fe^0 water filters and are both empirical relationships. It is essential to notice that the corrosion rate (k_{iron}) is not investigated as a function of the amount of individual corrosive species (e.g., Cl^-, contaminants, H_2S), but rather as the extent of iron corrosion as influenced by these and all other operational parameters (flow velocity, system design, temperature). In other words, considering that contaminants are the main corroding agents for Fe^0 is alien to corrosion science [10,13,14,25,40,41].

2.2. Corrosion Rate and Extent of Mass Loss

The extent of aqueous Fe^0 corrosion under environmental conditions is generally expressed either in terms of [40,41] (i) the change in Fe^0 weight (mass loss), (ii) the dimensions of the corroded crevices, (iii) the number and quantity of formed pits or (iv) the amount of corrosion products (e.g., the thickness of the oxide scale; Equations (7)–(9)). Equation (10) expresses the corrosion rate (k_{iron}) in terms of mass loss:

$$k_{iron} = K \times \frac{mb - ma}{A} \times \rho \times t \quad (10)$$

where k_{iron} (mm/y) is the corrosion rate; m_b (g) is the mass before exposure; m_a (g) is the mass after exposure; A (mm^2) is exposed surface area; t (years) is the exposure time; ρ (g/cm^3) is density and K a constant. Expressing the time in years suggests that, to be relevant, experiments should ideally last for several years.

Another conventional way to access k_{iron} uses the Faraday law. Here, k_{iron} is quantified through the relationship between the corrosion current density and the extent of metal dissolution [41,42].

2.3. Oxide Scale Formation and Its Effects on k_{iron}: Modeling Aspects

Equation (10) shows that k_{iron} depends on $\Delta m = m_b - m_a$, A and t. Δm is related to the amount of corrosion products within the system or the thickness of the oxide scale (x value; Equations (7)–(9)). The time-dependent changes of Δm and A render corrosion processes very complex. Generally, one should consider the following processes [40,41,43]: (i) the Fe^0 dissolution (anodic reaction) at the free metal surface; (ii) water reduction (cathodic reaction) at the Fe^0 surface; (iii) the precipitation equilibria yielding the oxide scale on the Fe^0 surface; (iv) the dissolution of the oxide scale (abiotic and biotic); (v) chemical reactions within the oxide scale (including Equations (3) and (4)); (vi) adsorption, co-precipitation and mass transfer across and within the oxide scale; and (vii) electro-migration (ionic transport) through the oxide-scale. The latter depends on the permeability and the surface charge of the precipitates building the scale [43].

A comprehensive model for the corrosion process should take into account all of these phenomena. Such a model would contain a large number of parameters. Relevant parameters could not be unequivocally determined on the basis of the limited amount of data that is available in the literature. This is an argument for new, holistic and systematic investigations. However, appropriate simplifications could be made. For example, Anderko and Young [44] considered that separate species form on the corroding Fe^0 surface in order to derive a mathematical model that represents the effects of scale formation on corrosion rates. The time-dependent change of each Fe^0 surface fraction is mathematical expressed. Similarly appropriate assumptions could be made on the reaction orders, the absorption behavior (e.g., Freundlich, Langmuir) and all other relevant aspects [44,45].

The approach conventionally used in the Fe^0 water filtration literature [16,19,27–30] is not derived from Equation (10) and related simplifications. Moreover, the presentation above reveals that chemical reactions yielding contaminants reductive transformation in Fe^0/H_2O systems (Equations (3) and (4)) are included in just one of seven processes making up the dynamics of oxide scale formation and transformation. For this reason, it would be difficult to find a model really describing an actual Fe^0/H_2O system within the remediation literature.

3. Metallic Iron for Water Treatment

3.1. Major Characteristics of Fe^0 Materials for Water Filters

Reactive Fe^0 materials used for water filters are characterized mostly by their size/thickness of less than 5.0 mm [46–49]. A widely-used Fe^0 sample from iPuTech (Rheinfelde, Germany) has a grain size varying from 0.3 to 2.0 mm [16,47]. This diameter represents less than 1/10 of the thickness of the buried cast iron pipes investigated by Mohebbi and Li [50]. The pipe presented pits having widths varying from 13 to 117 mm and depths from 1.6 to 9.1 mm after a service life of 90 years. From the study of Mohebbi and Li [50], an average rate constant (k_{iron}) for a cast iron pipe under service conditions can be derived (Equation (10)), but such k_{iron} values cannot be extrapolated to Fe^0 materials for water filters, even when they result from the same cast iron. Many material and application-dependent k_{iron} values can be found in the broad literature [51,52] using Fe^0, but none of them can be adopted for Fe^0 filters. Relevant fields include metal recovery by the cementation process, which was established in 1890s [53,54]. In the cementation process, metal (e.g., Fe^0, Zn^0) particles are used in technical devices for some weeks or months and the major (controlled) operating conditions (e.g., high temperatures or low pH values) are not comparable to those of water filters. In particular, high metal ion concentrations warrant the formation of an electronic conductive layer of recovered metals at the Fe^0 surface, while in the water filtration industry, a multi-layered, nonconductive oxide scale ("passive" film) is inevitably formed [55], rendering quantitative direct reduction (electrons from Fe^0) simply impossible.

3.2. Coping with the Singularity of Fe^0 Filters

In order to assess the service life of Fe^0 filters, it is imperative to determine corrosion rates (k_{iron}) of relevant Fe^0 materials over the long term and to develop models for Fe^0 depletion to be correlated with the extent of contaminant removal under operational conditions. Although many studies have been performed to determine the rate constant of the degradation (chemical reduction) of individual contaminants ($k_{contaminant}$; based on reactions similar to Equation (1)) (Section 2), little research has been undertaken, which could be used to derive k_{iron} values over longer time scale than days, weeks or a few months. The intention herein is to pave the way to fill the gap regarding the long-term corrosion rate of materials for Fe^0 filters in the absence of historical data. Clearly, long-term experiments for the determination of k_{iron} values are urgently needed to assist the development of reliable models to predict the service life of Fe^0 filters and/or describe their operation.

It is understood that the k_{iron} value is not an intrinsic property of the material, but depends on several inter-related site-specific parameters. For example, the same material will exhibit different k_{iron} values in reactive zones containing the same amount of Fe^0, but having different volumetric Fe^0:sand ratios, e.g., 10:90, 25:75 and 50:50. The rationale is that the long-term kinetics of iron corrosion also depends on the pressure within the filter (P_{H2} in Equation (6)). The initial k_{iron} value (k^0_{iron}) could be identical in the three systems, but with increasing service life, systems with higher Fe^0 ratios will exhibit lower k_{iron} values. Remember that in designing Fe^0 filters, the goal is to work with the material, for which k_{iron} value implies efficient decontamination under the operational conditions (e.g., bed thickness, flow velocity, water chemistry). Clearly, selecting an appropriate material for a given site is not seeking for the most reactive one.

4. Modeling Permeability Loss of Fe^0 Filters

4.1. Lessons from Monitored Aquifer Recharge

In many regions of the world, monitored aquifer recharge (MAR) is applied as a tool to (i) overcome the over-exploitation of groundwater or (ii) store excess storm water in the subsurface [56,57]. While injecting water into an aquifer, clogging does often occur, possibly rendering MAR inefficient in the long-term. There are three clogging types: (i) biological clogging due to growing biofilms; (ii) chemical clogging due mostly to precipitation reactions; and (iii) physical clogging caused by suspended solids. In many cases, it has been demonstrated that physical clogging accounts for about 70% of the permeability loss [58].

A particular case of water injection into the aquifer is that of the re-circulation of iron-rich groundwaters. Here, the precipitation of Fe^{II}/Fe^{III} mineral phases significantly reduces the porosity of the aquifer system after a certain operation duration. The removal of dissolved iron by several techniques was proven efficient in sustaining MAR operations [59]. In the context of Fe^0 filters, dissolved iron generates and precipitates within the system (*in situ*). Accordingly, dissolved iron cannot be removed, but only properly considered. Thus, the two major lessons from the MAR technology are that: (i) suspended substances should be filtered out; and (ii) the generation, migration and transformation of Fe species should be carefully considered (mass balance, including volumetric expansion).

4.2. Lessons from the Merrill-Crowe Process

The century-old zinc cementation for gold recovery from a pregnant leach liquor (the Merrill-Crowe process) reveals that clarification and deaeration (O_2 removal) of the leach liquor are two decisive stages to optimize the efficiency of Fe^0 filters. Clarification corresponds to the elimination of suspended substances (Section 4.1) to avoid physical clogging.

In its original version, the cementation process involved the filtration of a gold-bearing cyanide solution through a packed bed of zinc shavings. This operation was proven to have little efficiency because the reaction rate was very slow and the Zn^0 surface was soon "passivated". The problem of

passivation was solved by the addition of a lead salt (e.g., $Pb(NO_3)_2$). This allowed a Zn^0/Pb^0 bimetallic system to form at the Zn^0 surface (shavings), enabling continued gold cementation (deposition).

Two further improvements were realized later: (i) using zinc dust rather than shavings; and (ii) the deaeration of the gold-bearing solution to O_2 levels lower than 1.0 mg L^{-1}. Zn^0 dust provided a much larger surface area ("A" in Equation (10)) for gold precipitation (Equation (11)), while the deaeration significantly reduced Zn^0 consumption through O_2. Clearly, a concurrent reaction for Zn^0 consumption is eliminated.

$$Zn^0 + Au^{2+} \Rightarrow Zn^{2+} + Au^0 \quad (11)$$

Replacing Zn^0 by Fe^0, in the context of Fe^0 filters, iron corrosion by water (Equation (2)) is the main reaction and corresponds to Equation (11).

It has been established that disturbance through dissolved O_2 results from the acceleration of Equation (2) by consumption of Fe^{II} species that are the effective reducing agents for O_2. Considering permeability loss, Fe^0 corrosion in the presence of O_2 yields more voluminous Fe^{III} oxides (e.g., Fe_2O_3, FeOOH) and hydroxides (Table 1). Table 1 summarizes the densities of iron corrosion products and the corresponding coefficient of volumetric expansion. If it is assumed that all oxidized Fe remains in the system (no transport of Fe^{II}/Fe^{III}), then it becomes evident that, for a constant volume (initial porosity of a Fe^0 filter), the systems with more oxygen will clog early [7,60].

Table 1. Theoretical ratios (η values) between the volume of expansive corrosion products (V_{oxide}) and the volume of iron consumed during the corrosion process (V_{Fe}). η values are compiled by Caré *et al.* [60]. The ratios of ρ values (densities) indicate that corrosion products are 1.5 to 2.2 times larger in volume than the parent Fe^0.

Species	Formula	ρ (kg m^{-3})	ρ_{iron}/ρ_{oxide}	V_{oxide}/V_{iron}
Iron	Fe	7800	–	–
Hematite	Fe_2O_3	5260	1.5	2.12
Magnetite	Fe_3O_4	5180	1.5	2.08
Goethite	α-FeOOH	4260	1.8	2.91
Akageneite	β-FeOOH	3560	2.2	3.48
Lepidocrocite	γ-FeOOH	4090	1.9	3.03

The logical consequence of the presentation above is that the use of O^{2-} poor leach liquors is a prerequisite for efficient Au recovery through Zn^0 cementation in packed beds. This process is ultimately known as the Merrill-Crowe precipitation process. Coming back to Fe^0 filters, it becomes evident that the analysis of the chemistry of the system would have enabled the proper consideration of the volumetric expansive nature of iron corrosion (Table 1) prompted at the start of the technology some 25 years ago.

The major lesson from the Merrill-Crowe precipitation process for Fe^0 filters is that controlling the O_2 level is essential for the efficiency of a filter. O_2 accelerates corrosion and can be beneficial in some cases. Where necessary, even stronger oxidizing agents can be used [32,61]. However, it should be carefully considered that more corrosion products implies rapid clogging, such that it is certain that long-term permeable systems should operate at low O_2 levels.

4.3. Conventional Approach

Conventionally, numerical models are used to predict the long-term behavior of Fe^0 filters (see [19] and the references cited therein). Data for such models should be derived from well-designed laboratory column experiments performed under operational conditions (e.g., experimental duration, flow velocity, temperature and water chemistry) mimicking as closely as possible those expected in the field. However, such studies currently provide at best information for understanding the early service life of Fe^0 filters (some months). In fact, experiments lasting for more than one year are very

scarce [19,62,63], while it is not established that k_{iron} determined under such conditions would describe the behavior of Fe^0 filters for 10 or 15 years. Moreover, according to Alamilla *et al.* [51], it is even not likely that this will be the case because of the well-documented non-linearity of the kinetics of iron corrosion [64] (Section 2).

It has been unambiguously demonstrated that all tools used to accelerate lab-scale experiments collectively impair the reliability of the obtained test results [35,65–67]. Relevant tools include adding oxidizing agents to accelerate corrosion [58], increasing flow velocity [34] and using Fe^0 of smaller particle sizes and/or rapid small-scale column tests [65]. For the early phase of column operation, methylene blue (MB) discoloration has been proven a powerful indicator of reactivity [68–74]. Actually, the longest experiment with MB in this context lasted only for months [69]. Accordingly, the suitability of MB discoloration for characterizing the long-term behavior of Fe^0 filters is yet to be investigated.

While the reliability of data currently used to model processes in Fe^0 filters is questioned, there is evidence that used k_{iron} values are inaccurate. For example, Moraci *et al.* [19] critically reviewed available approaches and presented a new modeling tool to simulate the permeability loss in Fe^0 filters. The presented model takes into account: (i) the volumetric expansive nature of iron corrosion; (ii) the precipitation of foreign species; and (iii) gas formation. However, a look at the used k_{iron} values suggests that there are still misunderstandings to be addressed before acceptable models are presented.

4.4. An Alternative Approach

The process of permeability loss should be investigated at the micro-scale [35]. The size of the Fe^0 particles, the volume of the space between individual grains and their modifications with the service life of the filter should be simultaneously considered.

4.4.1. Descriptive Aspects

Spherical Fe^0 particles are considered. Each particle has an initial diameter of d_0 ($t_0 = 0$). At $t > t_0$, the residual diameter of the particle (non-corroded Fe^0) is d. The *in situ* generated amount of corrosion products corresponds to $\Delta d = d_0 - d$. The initial mass of each particle is $m_p = \rho_{iron} \times V_0$ ($V_0 = \pi \times {d_0}^3/6$) A certain Fe^0 mass (m_0) is made up of N_0 particles, such that $m_0 = N_0 \times \rho_{iron} \times \pi \times {d_0}^3/6$. Assuming uniform corrosion, all N_0 particles corrode with the same kinetics (k_{iron}). At each time (t), the mass of non-corroded Fe^0 can be determined and the corresponding decrease in diameter (Δd) deduced. The average corrosion rate is given by Equation (12). The best scenario is the one in which Δd is directly measured (*in situ*).

$$k_{iron} = \Delta d/t \quad (12)$$

The surface area of a Fe^0 particle (A_p) with a diameter d is given by Equation (13):

$$A_p = \pi \times d^2 \quad (13)$$

The number of Fe atoms covering A_p can be deduced using Equation (14), while considering that each Fe atom (r_{atom} = 1.24 Å or d_{atom} = 2.48 Å) covers an effective area equal to a square (${d_{atom}}^2$).

$$N_A = A_p/{d_{atom}}^2 \quad (14)$$

This reasoning has intentionally ignored the evidence that isolated Fe^0 atoms do not exist; instead, each unit cell of Fe^0 (BCC) contains two (2) Fe atoms.

One major challenge for the Fe^0 filtration technology has been to properly consider the contribution of (volumetric expansive nature of) iron corrosion to permeability loss [16,33–35,75]. That is coupling Δd to the diminution of the porosity (Challenge 1). Challenge 1 has been resolved using mass balance equations [7,8,35,76]. For example the porosity loss or the residual porosity can be evaluated for several d values, e.g., $d_0/2$, $d_0/4$, $d_0/8$, $d_0/16$, $d_0/32$, $d_0/64$ . . . , $d = 0$ at t_∞. The

open question (Challenge 2) is how to correlate this spatial porosity loss to the service life of Fe^0 filters (temporal porosity loss). Thus, determining k_{iron} is the key to model the operation of Fe^0 filters. In the context of Fe^0 filters, "permeability loss" and "porosity loss" can be randomly interchanged as permeability loss is mostly mediated by the occupation of the inter-granular pore space (porosity) and, thus, to reduced interconnectivity of available pores (physical clogging). This is the reason why the entrance zone of a filter comparatively experiences increased porosity loss as a rule. This evidence alone makes the discussion of common column parameters like Reynold or Peclet numbers a complex task.

4.4.2. On the Significance of k_{iron} Values

The k_{iron} values used by Moraci *et al.* [19] as calibration parameters are expressed in mmol kg^{-1} d^{-1}. According to the references cited by these authors, such expressions are common in the Fe^0 literature. Each k_{iron} value should be given in mmol $particle^{-1}$ d^{-1}. The reason being that all Fe^0 particles are corroded by water (H^+ or H_2O) with the same kinetics. Admittedly, in the entrance zone, dissolved O_2 and/or other oxidizing agents, including contaminants (e.g., Cu^{II}, Cr^{VI}, NO_3^-) and co-solutes (e.g., Ca^{2+}, Cl^-, NO_3^-), will accelerate iron corrosion and, thus, the extent of permeability/porosity loss. However, permeability loss due to Equation (2) [7,9,33–35] is ideally uniform. For example, a k_{iron} value of 30 mmol kg^{-1} d^{-1} corresponding to 1680 mg kg^{-1} d^{-1} implies a daily dissolution of 1.57×10^{-2} mmol or 0.88 mg of iron from individual spherical particles having a diameter of 1.0 mm (d value). The equations used for calculations are summarized in the previous section, and the results of all k_{iron} values used by Moraci *et al*. [19] are summarized in Table 2.

Table 2. Values of k_{iron} used by Moraci *et al.* [19] and the corresponding t_∞ values. Calculations are made for d = 1.0 mm and m = 1 kg.

k_{iron} (mmol kg^{-1} d^{-1})	k_{iron} (mg kg^{-1} d^{-1})	k_{iron} (µg $particle^{-1}$ d^{-1})	t_∞ (years)
0.7	39	0.02	69.8
1.2	67	0.04	40.7
1.5	84	0.04	32.6
4.0	224	0.12	12.2
7.0	392	0.21	7.0
10.0	560	0.29	4.9
12.0	672	0.35	4.1
15.0	840	0.44	3.3
21.0	1176	0.62	2.3
30.0	1680	0.88	1.6
170.0	9520	4.99	0.3
200.0	11,200	5.87	0.2
242.0	13,552	7.10	0.2
300.0	16,800	8.80	0.2

Table 2 also summarizes the time to complete material depletion or Fe^0 exhaustion (t_∞) for the k_{iron} values used by Moraci *et al*. [19] assuming uniform corrosion for d = 1.0 mm. It is seen that t_∞ varies from 0.2 to 69.1 years. Keeping in mind that subsurface Fe^0 reactive walls (Fe^0 filters) should have a service life in the range of decades, Table 2 suggests that, for d = 1.0 mm, a material exhibiting a k_{iron} value averaging 4.0 mmol $particle^{-1}$ d^{-1} should be used. Such a material would last for 12.22 years (t_∞ value). These calculations suggest that in a cross-disciplinary approach, a challenge for material scientists (Challenge 3) would be to manufacture a (possibly porous) spherical material with a 1.0 mm diameter exhibiting an average of 0.12 µg $particle^{-1}$ d^{-1}. The same reasoning suggests that a material exhausting within one year (t_∞) should have a k_{iron} value of 1.47 µg $particle^{-1}$ d^{-1}. Such a material could be useful for household water filters [77].

It is understood that solving Challenge 3 will just be the first step in designing Fe^0 filters. In fact, the target k_{iron} value (e.g., 4.0 mmol $particle^{-1}$ d^{-1}) depends on a myriad of operational parameters,

including the porosity of the Fe^0 materials, the Fe^0 ratio in the reactive layer, the nature of the admixing aggregates (e.g., MnO_2, pumice, sand, TiO_2), the water flow velocity (residence time), the water chemistry (the composition of the electrolyte) and the thickness of the reactive layer. The next section proposes an approach for a systematic investigation yielding suitable materials for Fe^0 filters.

Table 3 and Figure 1 summarize the trend of the expected changes in efficiency as a function of *d* values. It is seen that the number of particles decreases exponentially with increasing *d* values, while the number of atoms at the surface increases. The objective of this communication is to outline that the law of efficiency change as d_0 changes to *d* in a Fe^0 filter is not yet established.

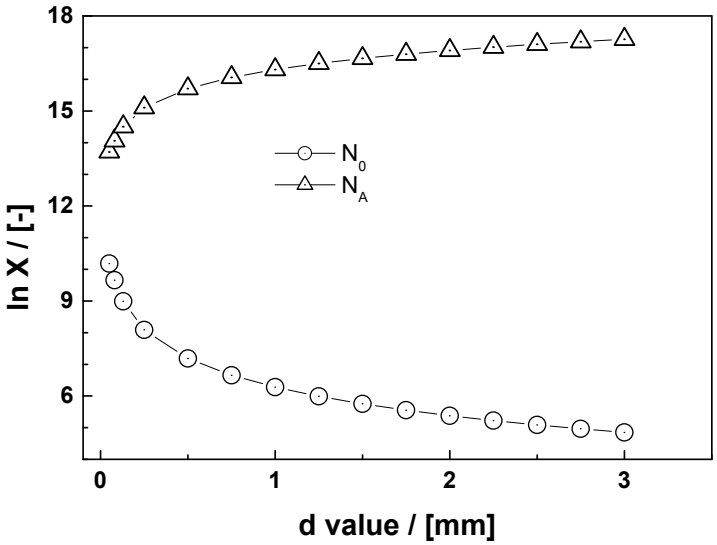

Figure 1. Changes of the number of particles (N_0) making up 1 kg of Fe^0 and the corresponding number of atoms at the surface (N_A) as a function of the d values. While the N_0 values exponentially decrease with increasing *d*, the N_A values increase.

Table 3. Values of the number of particles (N_0) making up 1 kg of Fe^0 as a function of the d values. The corresponding particle area (A_P) and the number of atoms at the surface (N_A) are specified.

d (mm)	N_0	A_p (m²)	N_A	N_A (µmol)
0.05	1.53×10^{10}	7.86×10^{7}	5.1×10^{13}	8.48×10^{-5}
0.08	4.53×10^{9}	1.77×10^{-6}	1.1×10^{14}	1.91×10^{-4}
0.13	9.77×10^{8}	4.91×10^{-6}	3.2×10^{14}	5.30×10^{-4}
0.25	1.22×10^{8}	1.96×10^{-5}	1.3×10^{15}	2.12×10^{-3}
0.50	1.53×10^{7}	7.86×10^{-5}	5.1×10^{15}	8.48×10^{-3}
0.75	4.53×10^{6}	1.77×10^{-4}	1.1×10^{16}	1.91×10^{-2}
1.00	1.91×10^{6}	3.14×10^{-4}	2.0×10^{15}	3.39×10^{-2}
1.25	9.77×10^{5}	4.91×10^{-4}	3.2×10^{15}	5.30×10^{-2}
1.50	5.66×10^{5}	7.07×10^{-4}	4.6×10^{15}	7.64×10^{-2}
1.75	3.56×10^{5}	9.63×10^{-4}	6.3×10^{15}	1.04×10^{-1}
2.00	2.39×10^{5}	1.26×10^{-3}	8.2×10^{15}	1.36×10^{-1}
2.25	1.68×10^{5}	1.59×10^{-3}	1.0×10^{15}	1.72×10^{-1}
2.50	1.22×10^{5}	1.96×10^{-3}	1.3×10^{15}	2.12×10^{-1}
2.75	9.18×10^{4}	2.38×10^{-3}	1.5×10^{15}	2.57×10^{-1}
3.00	7.07×10^{4}	2.83×10^{-3}	1.8×10^{15}	3.05×10^{-1}

5. Designing Long-Term, Efficient Fe^0 Filters

5.1. The Problem

The main problem of the Fe^0 filtration technology is the lack of appropriate standard tools to characterize the reactivity of used materials [47–49]. In other words, ill-defined materials have been used by various research groups and remediation companies for the past two decades. Accordingly, it is not surprising that only highly qualitative results have been presented. Considering this vacuity, the intention herein is to pave the way for the determination of k_{iron} values useful for modeling purposes. Clearly, while determining k_{iron} values useful for models, experiments should be designed to characterize as much parameters as possible in a systematic approach [77,78]. The major advantage of this approach is that the same set of experiments will generate data enabling the discussion of the appropriateness of current approaches, as well. For example, in a three-contaminant system employing arsenic, fluoride and uranium, the correlation of k_{iron} values to the time-dependent extent of the removal of each contaminant can be properly discussed. In a similar way, repeating the experiments of Luo *et al.* [34] for the long term will enable the determination of k_{iron} of the same sample in deionized water, groundwater and acid mine drainage (AMD).

In the absence of a reference material, an operational reference can be selected; for example, one of the materials commercialized by iPuTech mbH (Rheinfelde, Germany) and widely used in laboratory and field studies [47,79]. A material scientist solving Challenge 3 would manufacture Fe^0 materials to be characterized (k_{iron} values) and compared to the operational reference. Following this approach, available Fe^0 materials could be classified according to their k_{iron} values, which are only indirectly correlated to the intrinsic reactivity. It is understood that neither the reference nor one of the individual materials could be the material for all situations. The objective is to come out with various materials exhibiting various k_{iron} values, such that selection to meet site-specificity would be simplified. Section 4.3 suggested for Fe^0 materials with a 1.0 mm diameter, k_{iron} = 0.12 µg particle^{-1} d^{-1} is suitable for subsurface-reactive Fe^0 walls, whereas k_{iron} = 1.47 µg particle^{-1} d^{-1} is suitable for household water filters.

5.2. Ways to Reliable k_{iron} Values

A proven tool to determine k_{iron} values is to allow Fe^0 materials (initial diameter d_0) to corrode under specific conditions and to determine the time-dependent variation of either (i) the residual diameter (d) or (ii) the amount of generated corrosion product (corresponding to $\Delta d = d_0 - d$). The latter can be also expressed by the thickness of the oxide scale (x in Equations (7) to (9)). In essence, a good estimation can be realized by just weighing the dried materials at the start (t_0) and the end (t_∞) of the experiments (mass balance) [80]. In this approach, $\Delta m = m_\infty - m_0$ represents (approximately) the mass of generated corrosion products when the column is flushed by deionized water. Depending on the operational conditions (oxic/anoxic), reliable assumptions can be made on the nature of corrosion products to enable modeling porosity loss. If the system is flushed by other solutions, the mass balance of individual species must be considered. Proper assumptions on all reactions likely to occur in the system and their contribution to changes in porosity must be made.

Recent data have proven that (i) the residual diameter (d), (ii) the amount of generated corrosion products and (iii) the nature of corrosion products can be determined by *in situ* measurements/observations of both d and changes in the pore diameters [34]. In their excellent work using X-ray computed tomography (RX-CT), Luo *et al.* [34] used three different model waters: (i) distilled water, (ii) synthetic groundwater and (iii) synthetic AMD. Luo *et al.* [34] also investigated the impacts of three different Fe^0/sand ratios (w/w): 10:90, 50:50 and 100:0. Duplicating the experiments of Luo *et al.* [34] for longer experimental durations and more applicable experimental set-ups (for water treatment) will certainly allow the determination of reliable k_{iron} values for predictive models. In this effort, a pure Fe^0 column (100 % Fe^0) could be used just as a tool to shorten the experimental duration or as a negative reference. For long-term basic experiments, a volumetric Fe^0:aggregate ratio

of 25:75 should be used. Such experiments should not be stopped because contaminant breakthrough has occurred. In fact, the focus herein is on the efficiency of tested Fe^0 materials [69,71,72] and possibly characterizing the time to Fe^0 exhaustion (t_∞). There is certainly an infinity of possibilities of experimental designs; the present effort will be limited to two approaches: (i) the sampling-port approach (in one column); (ii) the column-in-series approach.

5.2.1. The Sampling-Port Approach

Experiments could be performed with a single column (ID = 5.0 cm, L > 50 cm) having a reactive zone (Fe^0-bearing) of 50 cm and equipped with five (5) sampling ports S_1, S_2, S_3, S_4 and S_5 at 10, 20, 30, 40 and 50 cm from the inlet, respectively (Figure 2). The influent solution is pumped upwards from a reservoir and at pre-defined time intervals. Effluents from each sample port are analyzed for pH value, dissolved iron, dissolved oxygen and concentrations of contaminants and co-solutes (e.g., Ca^{2+}, Cl^-, HCO_3^-, $H_2PO_4^-$, SO_4^{2-}). In addition to aqueous analysis, time-dependent changes of the morphology of Fe^0 and the pore structure should be documented by RX-CT, for example at the following distances from the inlet: 5 (S'_1), 15 (S'_2), 25 (S'_3), 35 (S'_4) and 45 cm (S'_5) of the reactive zone.

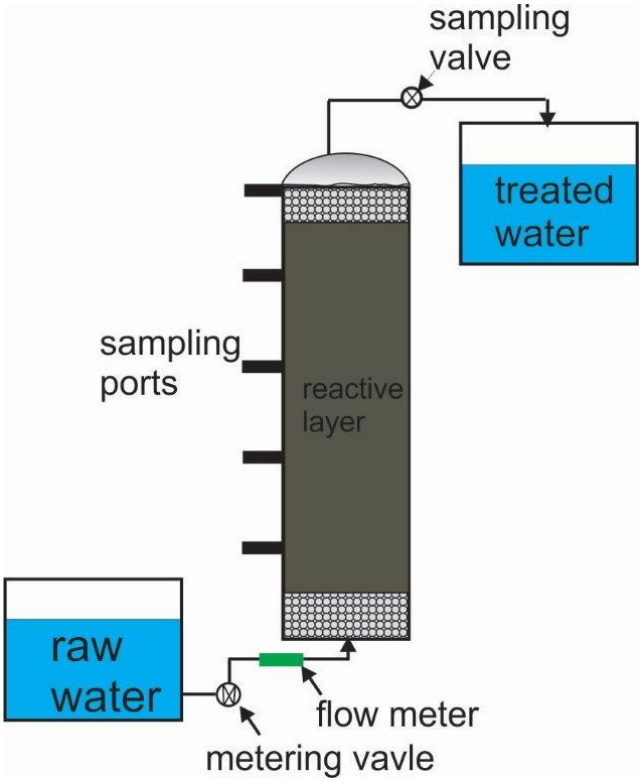

Figure 2. Side view of a single Fe^0/sand water filter comprising five sampling ports. To optimize the efficiency of the filtration unit, the effluent should be clarified and deaerated before being introduced into the first column. A simple device for clarification and deaeration is a slow sand filter [78].

This approach enables a reliable characterization of processes implying the well-documented increased porosity loss in the entrance zone of the Fe^0 filters (e.g., at S_1 *vs.* higher S_i stations) and how it is influenced by the presence of oxidizing agents (e.g., Cr^{VI}, dissolved O_2) in the influent solution. Moreover, by individually varying the influent O_2 concentration and other oxidizing agents, while monitoring its profile in the whole column (S_1 through S_5), a better discussion of its impact on the porosity loss is realized. The last important feature from this experimental approach is that, before O_2 breakthrough at S_4, the porosity loss at S'_5 is attributed solely to corrosion through water (Equation (1)) under the experimental conditions (anoxic conditions). Accordingly, by purposefully varying the

composition of influent solution, the impact of relevant operational parameters (e.g., Cl^-, HCO_3^-, SO_4^{2-}) on the extent of porosity loss through water can be characterized.

In the absence of RX-CT, or complementary to this tool, other approaches for monitoring changes of the water flow velocity at individual sample ports can be used. The reduction of the pore size is then deduced from the Darcy equation. At the end of the experiments (at least two years), the column is dismantled after the last RX-CT analysis, and the non-corroded Fe^0 materials and the corrosion products are characterized by various analytical tools, including selective extraction. This effort characterizes the changes of the following parameters as a function of the distance from the inlet: (i) the extent of Fe^0 depletion (e.g., in %); (ii) the average size of non-corroded Fe^0; (iii) the nature, the abundance and the reactivity of individual corrosion products; and (iv) the extent of the reduction of pore sizes.

5.2.2. The Column-In-Series Approach

The sample-port approach requires some sophisticated equipment, including the column and the pump. For less equipped laboratories (e.g., in the developing world), this could be prohibitively expensive. For these situations, small research units could be made up of five shorter columns (e.g., *ID* = 5.0 cm; *L* = 30 cm) in series (Figure 3). Individual columns are mostly filled with sand and contain a 10 cm-thick reactive layer. In this embodiment, each column corresponds roughly to 10 cm of the sample-port approach (Figure 2). The larger sand mass between the reactive layers enables the characterization of the impact of *in situ*-coated sand on the filter's efficiency. For Columns 1 through 4, the effluent from one column is routed to the next through a tubing system comprising a sampling station/valve (Figure 3).

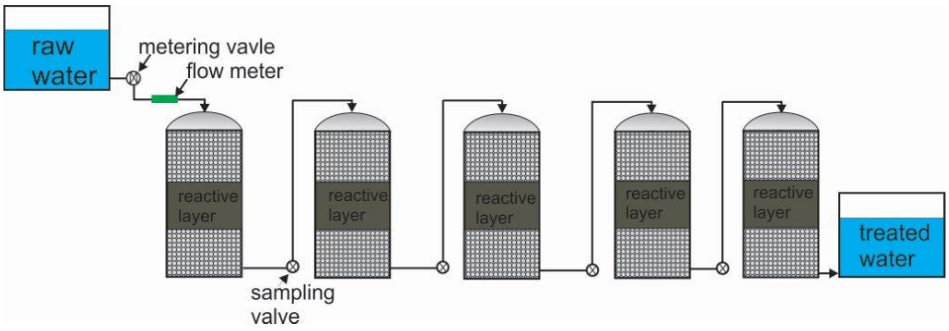

Figure 3. Side view of a series of the Fe^0/sand water filter comprising five individual columns and sampling valves. To optimize the efficiency of the filtration unit, the effluent should be clarified and deaerated before being introduced into the first column. A simple device for clarification and deaeration is a slow sand filter [78].

The results are exploited similarly as for the sample-port approach, the main objective being to determine the long-term kinetics of iron corrosion (k_{iron}). In this approach the system can be gravity fed. For example, it can be daily fed by 1000 mL of a model solution. For both approaches, the level of dissolved O_2 in the influent solution can be regulated by pre-filters: a relevant pre-filtration system is a slow sand filter (SSF) in which O_2 is consumed within a biofilm [81]. However, working with an SSF implies a low water flow velocity. Alternative approaches to decrease/lower the O_2 level include using a sacrificial Fe^0 column containing up to 10 vol% Fe^0 possibly of a smaller particle size. In fact, Fe^0 is a well-documented O_2 scavenger that is used in food packaging [82,83].

5.3. The Significance of the Short-Term Kinetics of Fe^0 Corrosion

The effort herein is to prepare the way for the determination of k_{iron} values of crucial importance for modeling scenarios to design long-term, efficient Fe^0 filters. Before being efficient for the long

term, however, Fe^0 filters have to be pre-conditioned in a "maturation" phase. Data from Kowalski and Sogaard [84] suggest that in their case, this maturation phase has lasted for six months. In the subsurface context, this means that the filtration system must contain short-term, efficient materials to assure contaminant removal in the initial service life of Fe^0 filters. Examples are adsorbents or more reactive Fe^0 materials, possibly with smaller particle sizes. The presentation above demonstrates that the short-term rate constants of Fe^0 corrosion (k^0_{iron}) have been mistakenly used to interpret results and/or to predict the behavior of long-term experiments. According to Alamilla *et al.* [51], the function describing the instantaneous rate of iron corrosion is expressed as follows:

$$v(t) = k_{iron} + (k^0_{iron} - k_{iron}) \times \exp(-q_0 \times t) \quad (15)$$

where q_0 is a constant, k^0_{iron} is the short-term and k_{iron} the long-term Fe^0 average corrosion rate. It can be seen that the instantaneous rate drops exponentially from k^0_{iron} to k_{iron} ($k^0_{iron} > k_{iron}$).

The real significance of k^0_{iron} values for subsurface Fe^0 filters is that materials should be selected such that after the initial rapid corrosion, the permeability of the reactive zone is still superior to that of the surrounding areas. If this condition is not satisfied, preferential flow would render the filter useless before the long-term corrosion rate (k_{iron}) is established.

While the short-term corrosion rate (k^0_{iron} value) is to be properly considered in designing subsurface Fe^0 filters, it could be sufficient to design some filters for the treatment of wastewaters from various sources (agriculture, industry, mine, residential area). Here, filters may be designed to operate just for some days to weeks, and material "regeneration" consists of just letting "used" materials be "activated" by humidity and air O_2 for a certain time before being re-used. k^0_{iron} values would be also sufficient to design several decontamination options using Fe^0 particles in batch or fluidized column systems. In this context, the system efficiency can be purposefully enhanced by using more or less powerful oxidizing agents [10,61], because bed clogging is not an important issue. All that is needed is increased Fe^0 corrosion to generate more contaminant scavengers [11,85,86]. k^0_{iron} values are also sufficient to design cementation beds for metal ion recovery.

6. Discussion

6.1. Contaminant Removal in Fe^0/H_2O Systems

The reliance of modelers on direct reduction by Fe^0 (electrons from the core metal) is not only of concern for modeling the long-term permeability of Fe^0 filters [3,87,88]. It strongly masks the real mechanisms of contaminant removal as that is a complex interplay between Fe^0 particles, Fe^{II} released into solution and Fe^{II}/Fe^{III} precipitation [89–96]. In particular, the transformation of Fe^0 to Fe oxides goes through colloids and hydroxides. The transformation "colloids to hydroxides" is accompanied by contaminants enmeshment (co-precipitation). In fact, whether they are reduced or not, contaminants are removed by adsorption, co-precipitation and size exclusion. On the other hand, regarding the abundance of (partly nascent) adsorbing sites and continuous generation of Fe^{II} species, contaminant chemical reduction by so-called structural Fe^{II} (adsorbed Fe^{II}) is favored [96]. The abundance of Fe^{II}/Fe^{III} hydroxides/oxides in Fe^0/H_2O systems has been experimentally demonstrated by [92]. However, the authors have suggested adsorptive removal as an important removal mechanism accompanying direct reduction, which is in contradiction to the mechanisms presented in Section 2. Accordingly, coming models for Fe^0/H_2O systems should be adjusted to address the main contaminant removal pathways.

6.2. The Shortcomings of Current Modeling Efforts

An overview of the Fe^0 filtration literature reveals conflicting information regarding the causes of permeability loss [7,75]. There is always a discrepancy between the observed and the predicted porosity loss; the actual porosity loss being higher than that predicted [75]. Two examples for illustration:

(i) Mackenzie *et al.* [82] measured a 5 to 10% porosity loss using tracer tests, while calculations based on mineral precipitation predicted only 1 %; and (ii) Kamolpornwijit and Liang [97] measured porosity losses of 25 to 30% based on tracer tests and attributed 1.3% to trapped gas. Mackenzie *et al.* [82] attributed the remaining porosity loss (up to 9%) to H_2 gas production. Henderson and Demond [75] realized that available models for Fe^0 filters [98–100] do not account for the effects of H_2 on permeability loss. In a series of carefully-designed experiments, Henderson and Demond [75] could validate their working hypothesis that the majority of porosity loss is not attributable to precipitates, but to gas.

The problem with the data of Henderson and Demond [75] is that they have not considered that each individual Fe^0 atom corrodes and produces both volumetric expansive precipitates and H_2 gas [35]. Moreover, the pore filling by Fe precipitates was evaluated using tabulated molar volume values (ν = 7.6 cm^3 mol^{-1} for Fe^0), which are not necessarily relevant for Fe^0 particles confined in a packed bed (Fe^0 filter). For example, the coefficient of volumetric expansion ($\eta = V_{oxide}/V_{iron}$) for magnetite ($Fe_3O_4$; ν = 45.0 cm^3 mol^{-1}) using ν values is 5.0, while the η value for confined system is close to 2.2 [60]. This combined with the lack of appropriate k_{iron} values has diminished the value of the models presented.

6.3. The True Value of Mathematical Modeling

Mathematical modeling constitutes the third pillar of science and engineering, achieving the fulfilment of the two more traditional disciplines: (i) theoretical analysis; and (ii) experimentation [101]. Mathematical models explore new solutions in a very short time period. This increases the speed of innovation cycles. However, this is only possible when theoretical analysis and experimentation are perfectly performed. The presentation herein has recalled that for Fe^0 filters, both theoretical analysis [102,103] and experimentation [104] have been unsatisfactory. This suggests that there is a huge gap between calculations and understanding [105]. Admittedly, all modelers are not chemists nor electrochemists, but even in the absence of a real cross-disciplinary approach, self-critical scientists should have realized that something fundamental is missing. Moreover, consultations with material and corrosion engineers would have been necessary in the fitness of things to save millions of money (mostly from tax payer) spent in intensive research on a biased basis. The damage is huge, as the credibility of modeling could be questioned [105]. This communication advocates for saving the credibility of mathematical modeling through the generation of credible data for Fe^0 filters.

The true value of mathematical models was recalled by Grauer [106] by the following wording: "theory and models cannot be validated in the strict sense but only refuted". The presentation herein has collectively refuted all modeling efforts regarding the design and operation of Fe^0 filters for the past two decades. The reason is the very poor theoretical analysis. The equation currently used for k_{iron} (corresponding to Equation (1)) is simply wrong, and the reductive transformation of contaminants is at best a side process (Equations (3) and (4)) (Section 2).

Better models are possible, they should be based on a systematic analysis of the Fe^0/H_2O system. A sound analysis [102,103] has demonstrated that contaminants are removed by adsorption, co-precipitation and size exclusion. Accordingly, chemical reduction when it occurs is not responsible for (quantitative) contaminant removal and is rather a side reaction occurring within the oxide scale in the vicinity of Fe^0 and not at its surface. The evidence that the surface of Fe^0 and oxides changes with time and the Fe^0 surface is not accessible to the contaminant question of the normalization of rate constants to the surface area [107]. Lastly, k_{iron} values are the pillar for modeling the temporal realization of permeability loss. These values are yet to be determined in well-designed long-term experiments.

6.4. Messages to Anonymous Collaborators

There is evidence in the Fe^0 literature that the aspects challenged herein are difficult to accept [108–112]. However, this argumentation corresponds to mainstream science (chemical thermodynamics). The first message to an anonymous collaborator (a reader) is "no single reference is

a quality guarantee". Accordingly, sound scientific arguments should justify each reference. Moreover, the rationale for preferring a work to another should be known and named, if applicable.

The second message is for a reviewer either for a submitted manuscript or a grant proposal. An author/applicant is a colleague and needs collegial remarks to improve his/her manuscript/proposal. A minimal requirement is that reviewer comments focus on points that need improvements or are unacceptable [113–115].

The third message is to the attention of funding agencies. Each applicant should have the opportunity to write some comments on the reviewer's evaluation before the final decision is made. This is of particular importance when the majority of available comments is negative. Admittedly, this could/would lengthen the review process, but this is the way to greater fairness. This procedure is already adopted by some agencies, but should be universally adopted. The reason is that the best evaluator could not recognize an innovation at first glance.

The fourth and last message is for everyone. Research on water treatment and environmental remediation has been wrongly directed from the beginning onward. Warnings from chemists [116–119] were simply ignored. Whenever a mistake is identified, starting on a new basis is always a good decision. Individual researchers already went down this path [10,119]. As an example, the author of this communication has published on reductive precipitation of U^{VI} by Fe^0 [120], then on reduction as a removal mechanism, until 2010 [14], only with [121] and hints from anonymous reviewers did he realize that at concentrations relevant for safe drinking water, reduction cannot be a stand-alone removal mechanism for any contaminant [78,122]. For environmental remediation, chemical reduction (degradation) may be sufficient when reaction products are readily degradable, for instance when nitrobenzene is quantitatively reduced to aniline. For safe drinking water provision, even reduction products (here, aniline) must be removed [123–126].

7. Concluding Remarks

Iron corrosion is a stochastic, probabilistic phenomenon that requires interdisciplinary concepts, including chemistry, electrochemistry, hydrodynamics, materials science, metallurgy, physics and surface science. From a pure chemical perspective, the thermodynamics and kinetics of the involved processes must be understood in order to effectively design and fabricate materials to be used for optimal (efficient and affordable) applications. This communication has recalled that the chemistry of the Fe^0/H_2O system is being incompletely considered while using Fe^0 as a remediation material. It is particularly disappointing/frustrating that the principles of corrosion as already understood and largely disseminated in the broad scientific literature have been simply ignored. The net result is that a fictive reaction (Equation (1)) has been used for dimensioning Fe^0 filters for more than two decades (25 years).

This communication has also recalled that mathematical modeling is the third and only the third pillar of science and technology. The two first pillars are theoretical analysis (system analysis) and experimentation. The best model will not correct mistakes in system analysis or experimentation. It is clear that Fe^0 filtration technology requires more accurate models that take into account the various mechanisms that underpin the process. The year-long experimentation on iron corrosion (prior to the advent of Fe^0 filters) has demonstrated that uniform corrosion assumed by almost all models is an over-simplification. In other words, even considering reliable values of k_{iron} will only describe how Fe^0 filters would behave considering the assumptions made (without biotic processes). This evidence confirms/suggests that (independent, where necessary) monitoring of the performance of Fe^0 filters is mandatory.

To conclude, Rolf Grauer will be paraphrased as follows: It would make more sense to devote more time and energy to determine k_{iron} values than to develop sophisticated, but unreliable numerical models. It is clearly understood that no particular Fe^0 material is a universal solution for all contaminations. Each and every case has to be considered in its totality before a decision is made on

the proper material, characterized by its k_{iron} value. Therefore, a sort of database for k_{iron} values is needed. Establishing such a database is a scientific challenge and not just laborious work.

Acknowledgments: Arnaud Igor Ndé-Tchoupé (Faculty of Sciences, University of Douala/Cameroon), Günther Meinrath (RER Consultants, Passau/Germany), Hans Rupprt (Department of Sedimentology & Environmental Geology, University of Göttingen), Hezron T. Mwakabona (Department of Physical Sciences, Sokoine University of Agriculture, Morogoro/Tanzania) and Mohammad Azizur Rahman (ISU, Leibniz University, Hannover/Germany) are thanked for their valuable advice. The manuscript was further improved by the insightful comments of anonymous reviewers from Water. The author acknowledges support by the German Research Foundation and the Open Access Publication Funds of the Göttingen University.

Conflicts of Interest: The author declares no conflict of interest.

Abbreviations

The following abbreviations are used in this manuscript:

AMD	acid mine drainage
ID	internal diameter
L	length (of the column)
MAR	monitored aquifer recharge
RX-CT	X-ray computed tomography
SSF	slow sand filter

References

1. Bartzas, G.; Komnitsas, K. Solid phase studies and geochemical modelling of low-cost permeable reactive barriers. *J. Hazard. Mater.* **2010**, *183*, 301–308. [CrossRef] [PubMed]
2. Li, L.; Benson, C.H. Evaluation of five strategies to limit the impact of fouling in permeable reactive barriers. *J. Hazard. Mater.* **2010**, *181*, 170–180. [CrossRef] [PubMed]
3. Obiri-Nyarko, F.; Grajales-Mesa, S.J.; Malina, G. An overview of permeable reactive barriers for *in situ* sustainable groundwater remediation. *Chemosphere* **2014**, *111*, 243–259. [CrossRef] [PubMed]
4. Statham, T.M.; Stark, S.C.; Snape, I.; Stevens, G.W.; Mumford, K.A. A permeable reactive barrier (PRB) media sequence for the remediation of heavy metal and hydrocarbon contaminated water: A field assessment at Casey Station, Antarctica. *Chemosphere* **2016**, *147*, 368–375. [CrossRef] [PubMed]
5. Noubactep, C.; Caré, S. Dimensioning metallic iron beds for efficient contaminant removal. *Chem. Eng. J.* **2010**, *163*, 454–460. [CrossRef]
6. Noubactep, C.; Caré, S. Designing laboratory metallic iron columns for better result comparability. *J. Hazard. Mater.* **2011**, *189*, 809–813. [CrossRef] [PubMed]
7. Caré, S.; Crane, R.; Calabrò, P.S.; Ghauch, A.; Temgoua, E.; Noubactep, C. Modeling the permeability loss of metallic iron water filtration systems. *Clear Soil Air Water* **2013**, *41*, 275–282. [CrossRef]
8. Rahman, M.A.; Karmakar, S.; Salama, H.; Gactha-Bandjun, N.; Btatkeu-K., B.D.; Noubactep, C. Optimising the design of Fe^0-based filtration systems for water treatment: The suitability of porous iron composites. *J. Appl. Solut. Chem. Model.* **2013**, *2*, 165–177.
9. Noubactep, C. Flaws in the design of Fe(0)-based filtration systems? *Chemosphere* **2014**, *117*, 104–107. [CrossRef] [PubMed]
10. Ghauch, A. Iron-Based Metallic Systems: An Excellent Choice for Sustainable Water Treatment. Ph.D. Thesis, Chemistry at Joseph Fourier University of Grenoble, Grenoble, France, December 2015.
11. Noubactep, C. Metallic iron for environmental remediation: A review of reviews. *Water Res.* **2015**, *85*, 114–123. [CrossRef] [PubMed]
12. Noubactep, C. Designing metallic iron packed-beds for water treatment: A critical review. *Clean Soil Air Water* **2016**, *44*, 411–421. [CrossRef]
13. Noubactep, C. Processes of contaminant removal in "Fe^0–H_2O" systems revisited: The importance of co-precipitation. *Open Environ. J.* **2007**, *1*, 9–13. [CrossRef]
14. Noubactep, C. A critical review on the mechanism of contaminant removal in Fe^0–H_2O systems. *Environ. Technol.* **2008**, *29*, 909–920. [CrossRef] [PubMed]

15. Noubactep, C. The fundamental mechanism of aqueous contaminant removal by metallic iron. *Water SA* **2010**, *36*, 663–670. [CrossRef]
16. Ulsamer, S. A Model to Characterize the Kinetics of Dechlorination of Tetrachloroethylene and Trichloroethylene by a Zero Valent Iron Permeable Reactive Barrier. Master's thesis, Worcester Polytechnic Institute, Worcester, UK, 2011.
17. Jeen, S.-W.; Yang, Y.; Gui, L.; Gillham, R.W. Treatment of trichloroethene and hexavalent chromium by granular iron in the presence of dissolved $CaCO_3$. *J. Contam. Hydrol.* **2013**, *144*, 108–121. [CrossRef] [PubMed]
18. Guan, X.; Sun, Y.; Qin, H.; Li, J.; Lo, I.M.C.; He, D.; Dong, H. The limitations of applying zero-valent iron technology in contaminants sequestration and the corresponding countermeasures: The development in zero-valent iron technology in the last two decades (1994–2014). *Water Res.* **2015**, *75*, 224–248. [CrossRef] [PubMed]
19. Moraci, N.; Ielo, D.; Bilardi, S.; Calabrò, P.S. Modelling long term hydraulic conductivity behaviour of zero valent iron column tests for PRB design. *Can. Geotec. J.* **2015**. [CrossRef]
20. Tratnyek, P.G. Putting corrosion to use: remediating contaminated groundwater with zero-valent metals. *Chem. Ind.* **1996**, *13*, 499–503.
21. Stratmann, M.; Müller, J. The mechanism of the oxygen reduction on rust-covered metal substrates. *Corros. Sci.* **1994**, *36*, 327–359. [CrossRef]
22. Jiao, Y.; Qiu, C.; Huang, L.; Wu, K.; Ma, H.; Chen, S.; Ma, L.; Wu, L. Reductive dechlorination of carbon tetrachloride by zero-valent iron and related iron corrosion. *Appl. Catal. B: Environ.* **2009**, *91*, 434–440. [CrossRef]
23. Ghauch, A.; Abou Assi, H.; Bdeir, S. Aqueous removal of diclofenac by plated elemental iron: Bimetallic systems. *J. Hazard. Mater.* **2010**, *182*, 64–74. [CrossRef] [PubMed]
24. Ghauch, A.; Abou Assi, H.; Baydoun, H.; Tuqan, A.M.; Bejjani, A. Fe^0-based trimetallic systems for the removal of aqueous diclofenac: Mechanism and kinetics. *Chem. Eng. J.* **2011**, *172*, 1033–1044. [CrossRef]
25. Gheju, M. Hexavalent chromium reduction with zero-valent iron (ZVI) in aquatic systems. *Water Air Soil Pollut.* **2011**, *222*, 103–148. [CrossRef]
26. Gheju, M.; Balcu, I. Removal of chromium from Cr(VI) polluted wastewaters by reduction with scrap iron and subsequent precipitation of resulted cations. *J. Hazard. Mater.* **2011**, *196*, 131–138. [CrossRef] [PubMed]
27. Jeen, S.-W.; Gillham, R.W.; Przepiora, A. Predictions of long-term performance of granular iron permeable reactive barriers: Field-scale evaluation. *J. Contam. Hydrol.* **2011**, *123*, 50–64. [CrossRef] [PubMed]
28. Jeen, S.-W.; Amos, R.T.; Blowes, D.W. Modelling gas formation and mineral precipitation in a granular iron column. *Environ. Sci. Technol.* **2012**, *46*, 6742–6749. [CrossRef] [PubMed]
29. Weber, A.; Ruhl, A.S.; Amos, R.A. Investigating dominant processes in ZVI permeable reactive barriers using reactive transport modeling. *J. Contam. Hydrol.* **2013**, *151*, 68–82. [CrossRef] [PubMed]
30. Firdous, R.; Devlin, J.F. BEARKIMPE-2: A VBA Excel program for characterizing granular iron in treatability studies. *Computer Geosci.* **2014**, *63*, 54–61. [CrossRef]
31. Lackovic, J.A.; Nikolaidis, N.P.; Dobbs, G.M. Inorganic arsenic removal by zero-valent iron. *Environ. Eng. Sci.* **2000**, *17*, 29–39. [CrossRef]
32. Gottinger, A.M.; McMartin, D.W.; Wild, D.J.; Moldovan, B. Integration of zero valent iron sand beds into biological treatment systems for uranium removal from drinking water wells in rural Canada. *Can. J. Civ. Eng.* **2013**, *40*, 945–950. [CrossRef]
33. Zhang, Y.; Gillham, R.W. Effects of gas generation and precipitates on performance of Fe^0 PRBs. *Ground Water* **2005**, *43*, 113–121. [CrossRef] [PubMed]
34. Luo, P.; Bailey, E.H.; Mooney, S.J. Quantification of changes in zero valent iron morphology using X-ray computed tomography. *J. Environ. Sci.* **2013**, *25*, 2344–2351. [CrossRef]
35. Domga, R.; Togue-Kamga, F.; Noubactep, C.; Tchatchueng, J.B. Discussing porosity loss of Fe^0 packed water filters at ground level. *Chem. Eng. J.* **2015**, *263*, 127–134. [CrossRef]
36. Reardon, J.E. Anaerobic corrosion of granular iron: Measurement and interpretation of hydrogen evolution rates. *Environ. Sci. Technol.* **1995**, *29*, 2936–2945. [CrossRef] [PubMed]
37. Reardon, J.E. Zerovalent irons: Styles of corrosion and inorganic control on hydrogen pressure buildup. *Environ. Sci. Technol.* **2005**, *39*, 7311–7317. [CrossRef] [PubMed]

38. Reardon, J.E. Capture and storage of hydrogen gas by zero-valent iron. *J. Contam. Hydrol.* **2014**, *157*, 117–124. [CrossRef] [PubMed]
39. Noubactep, C.; Meinrath, G.; Dietrich, P.; Sauter, M.; Merkel, B. Testing the suitability of zerovalent iron materials for reactive Walls. *Environ. Chem.* **2005**, *2*, 71–76. [CrossRef]
40. Nesic, S. Key issues related to modelling of internal corrosion of oil and gas pipelines-A review. *Corros. Sci.* **2007**, *49*, 4308–4338. [CrossRef]
41. Obuka, N.S.P.; Ikwu, O.N.C.; Chukwumuanya, G.R.O.; Okechukwu, E. Review of corrosion kinetics and thermodynamics of CO_2 and H_2S corrosion effects and associated prediction/evaluation on oil and gas pipeline system. *Int. J. Sci. Technol. Res.* **2012**, *1*, 156–162.
42. Wang, J.; Farrell, J. Investigating the role of atomic hydrogen on chloroethene reactions with iron using tafel analysis and electrochemical impedance spectroscopy. *Environ. Sci. Technol.* **2003**, *37*, 3891–3896. [CrossRef] [PubMed]
43. Noubactep, C.; Schöner, A.; Sauter, M. Significance of oxide-film in discussing the mechanism of contaminant removal by elemental iron materials. In *Photo-Electrochemistry & Photo-Biology for the Sustainability*; Bentham Science Publishers: Sharjah, UAE, 2010; pp. 97–122.
44. Anderko, A.; Young, R.D. Simulation of CO_2/H_2S corrosion using thermodynamic and electrochemical models. In Proceedings of NACE international Corrosion Annual Conference, San Antonio, TX, USA, 25–30 April 1999.
45. Anderson, A.B.; Ray, N.K. Structures and reactions of H_3O^+, H_2O, and OH on an Fe electrode. Potential dependence. *J. Phys. Chem.* **1982**, *86*, 488–494. [CrossRef]
46. Miehr, R.; Tratnyek, G.P.; Bandstra, Z.J.; Scherer, M.M.; Alowitz, J.M.; Bylaska, J. E. Diversity of contaminant reduction reactions by zerovalent iron: Role of the reductate. *Environ. Sci. Technol.* **2004**, *38*, 139–147. [CrossRef] [PubMed]
47. Btatkeu-K., B.D.; Miyajima, K.; Noubactep, C.; Caré, S. Testing the suitability of metallic iron for environmental remediation: Discoloration of methylene blue in column studies. *Chem. Eng. J.* **2013**, *215*, 959–968. [CrossRef]
48. Birke, V.; Schuett, C.; Burmeier, H.; Friedrich, H.-J. Impact of trace elements and impurities in technical zero-valent iron brands on reductive dechlorination of chlorinated ethenes in groundwater. In *Permeable Reactive Barrier Sustainable Groundwater Remediation*; Naidu, R., Birke, V., Eds.; CRC Press: Boca Raton, FL, USA, 2014; pp. 87–98.
49. Li, S.; Ding, Y.; Wang, W.; Lei, H. A facile method for determining the Fe(0) content and reactivity of zero valent iron. *Anal. Methods* **2016**, *8*, 1239–1248. [CrossRef]
50. Mohebbi, H.; Li, C.Q. Experimental investigation on corrosion of cast iron pipes. *Int. J. Corros.* **2011**, *2011*, 1–17. [CrossRef]
51. Alamilla, J.L.; Espinosa-Medina, M.A.; Sosa, E. Modelling steel corrosion damage in soil environment. *Corros. Sci.* **2009**, *51*, 2628–2638. [CrossRef]
52. Obanijesu, E.O.; Pareek, V.; Gubner, R.; Tade, M.O. Corrosion education as a tool for the survival of natural gas industry. *Nafta* **2010**, *61*, 541–554.
53. Habashi, F. A short history of hydrometallurgy. *Hydrometallurgy* **2005**, *79*, 15–22. [CrossRef]
54. Nicol, M.J.; Schalch, E.; Balestra, P.; Hegedus, H. A modern study of the kinetics and mechanism of the cementation of gold. *J. South African Inst. Min. Met.* **1979**, *79*, 191–198.
55. Noubactep, C. Elemental metals for environmental remediation: Learning from cementation process. *J. Hazard. Mater.* **2010**, *181*, 1170–1174. [CrossRef] [PubMed]
56. Dillon, P.; Pavelic, P.; Siebenaler, X.; Gerges, N.; Clark, R. Aquifer storage and recovery os stromwater runoff. *AWWA J. Water* **1997**, *24*, 7–11.
57. Rahman, M.A.; Wiegand, B.; Badruzzaman, A.B.M.; Ptak, T. Hydrogeological analysis of Upper Dupitila Aquifer towards the implementation of managed aquifer recharge project in Dhaka City, Bangladesh. *Hydrogeol. J.* **2013**, *21*, 1071–1089. [CrossRef]
58. Holländer, H.M.; Boochs, P.W.; Billib, M.; Panda, S.N. Laboratory experiments to investigate clogging effects in aquifers. *Grundwasser* **2005**, *10*, 205–215. (In German) [CrossRef]
59. Mutschmann, J.; Stimmelmayr, F. *Taschenbuch der Wasserversorgung*; Springer-Verlag: Stuttgart, Germany, 1991; p. 926.

60. Caré, S.; Nguyen, Q.T.; L'Hostis, V.; Berthaud, Y. Mechanical properties of the rust layer induced by impressed current method in reinforced mortar. *Cement Concrete Res.* **2008**, *38*, 1079–1091. [CrossRef]
61. Guo, X.; Yang, Z.; Dong, H.; Guan, X.; Ren, Q.; Lv, X.; Jin, X. Simple combination of oxidants with zero-valent-iron (ZVI) achieved very rapid and highly efficient removal of heavy metals from water. *Water Res.* **2016**, *88*, 671–680. [CrossRef] [PubMed]
62. Antia, D.D.J. Sustainable zero-valent metal (ZVM) water treatment associated with diffusion, infiltration, abstraction and recirculation. *Sustainability* **2010**, *2*, 2988–3073. [CrossRef]
63. Ruhl, A.S.; Weber, A.; Jekel, M. Influence of dissolved inorganic carbon and calcium on gas formation and accumulation in iron permeable reactive barriers. *J. Contam. Hydrol.* **2012**, *142*, 22–32. [CrossRef] [PubMed]
64. Taylor, C.D. Atomistic modeling of corrosion events at the interface between a metal and its environment. *Int. J. Corros.* **2012**, *2012*, 1–13. [CrossRef]
65. Zou, J.; Cannon, F.S.; Chen, W.; Dempsey, B.A. Improved removal of arsenic from groundwater using pre-corroded steel and iron tailored granular activated carbon. *Water Sci. Technol.* **2010**, *61*, 441–453. [CrossRef] [PubMed]
66. Bilardi, S.; Calabrò, P.S.; Caré, S.; Moraci, N.; Noubactep, C. Effect of pumice and sand on the sustainability of granular iron beds for the removal of CuII, NiII, and ZnII. *Clean Soil Air Water* **2013**, *41*, 835–843. [CrossRef]
67. Tepong-Tsindé, R.; Phukan, M.; Nassi, A.; Noubactep, C.; Ruppert, H. Validating the efficiency of the MB discoloration method for the characterization of Fe^0/H_2O systems using accelerated corrosion by chloride ions. *Chem. Eng. J.* **2015**, *279*, 353–362. [CrossRef]
68. Okwi, G.J.; Thomson, N.R.; Gillham, R.W. The impact of permanganate on the ability of granular iron to degrade trichloroethene. *Ground Water Monit. Remed.* **2005**, *25*, 123–128. [CrossRef]
69. Miyajima, K. Optimizing the design of metallic iron filters for water treatment. *Freib. Online Geosci.* **2012**, *32*, 60–61.
70. Miyajima, K.; Noubactep, C. Effects of mixing granular iron with sand on the efficiency of methylene blue discoloration. *Chem. Eng. J.* **2012**, *200*, 433–438. [CrossRef]
71. Btatkeu-K., B.D.; Olvera-Vargas, H.; Tchatchueng, J.B.; Noubactep, C.; Caré, S. Characterizing the impact of MnO_2 on the efficiency of Fe^0-based filtration systems. *Chem. Eng. J.* **2014**, *250*, 416–422. [CrossRef]
72. Phukan, M. Characterizing the Fe^0/sand system by the extent of dye discoloration. *Freib. Online Geosci.* **2015**, *42*, 80–86.
73. Phukan, M.; Noubactep, C.; Licha, T. Characterizing the ion-selective nature of Fe^0-based filters using azo dyes. *Chem. Eng. J.* **2015**, *259*, 481–491. [CrossRef]
74. Btatkeu-K., B.D.; Tchatchueng, J.B.; Noubactep, C.; Caré, S. Designing metallic iron based water filters: Light from methylene blue discoloration. *J. Environ. Manag.* **2016**, *166*, 567–573. [CrossRef] [PubMed]
75. Henderson, A.D.; Demond, A.H. Impact of solids formation and gas production on the permeability of ZVI PRBs. *J. Environ. Eng.* **2011**, *137*, 689–696. [CrossRef]
76. Noubactep, C.; Caré, S.; Crane, R.A. Nanoscale metallic iron for environmental remediation: Prospects and limitations. *Water Air Soil Pollut.* **2012**, *223*, 1363–1382. [CrossRef] [PubMed]
77. Tepong-Tsindé, R.; Crane, R.; Noubactep, C.; Nassi, A.; Ruppert, H. Testing metallic iron filtration systems for decentralized water treatment at pilot scale. *Water* **2015**, *7*, 868–897. [CrossRef]
78. Ndé-Tchoupé, A.I.; Crane, R.A.; Mwakabona, H.T.; Noubactep, C.; Njau, K. Technologies for decentralized fluoride removal: Testing metallic iron based filters. *Water* **2015**, *7*, 6750–6774. [CrossRef]
79. Trois, C.; Cibati, A. South African sands as a low cost alternative solution for arsenic removal from industrial effluents in permeable reactive barriers: Column tests. *Chem. Eng. J.* **2015**, *259*, 981–989. [CrossRef]
80. Glinka, N.L. *General Chemistry*; MIR Moscow: Leningrad, Russia, 1990. (In Russian)
81. Haig, S.-J. Characterising the Functional Ecology of Slow sand Filters through Environmental Genomics. Ph.D. Thesis, School of Engineering, University of Glasgow, Glasgow, UK, 2014.
82. Mackenzie, P.D.; Horney, D.P.; Sivavec, T.M. Mineral precipitation and porosity losses in granular iron columns. *J. Hazard. Mater.* **1999**, *68*, 1–17. [CrossRef]
83. Noubactep, C. Relevant reducing agents in remediation Fe^0/H_2O systems. *Clean Soil Air Water* **2013**, *41*, 493–502. [CrossRef]
84. Kowalski, K.P.; Søgaard, E.G. Implementation of zero-valent iron (ZVI) into drinking water supply-Role of the ZVI and biological processes. *Chemosphere* **2014**, *117*, 108–114. [CrossRef] [PubMed]

85. Bojic, A.; Purenovic, M.; Bojic, D. Removal of chromium(VI) from water by micro-alloyed aluminium based composite in flow conditions. *Water SA* **2004**, *30*, 353–359. [CrossRef]
86. Bojic, A.Lj.; Bojic, D.; Andjelkovic, T. Removal of Cu^{2+} and Zn^{2+} from model wastewaters by spontaneous reduction-coagulation process in flow conditions. *J. Hazard. Mater.* **2009**, *168*, 813–819. [CrossRef] [PubMed]
87. Sarr, D. Zero-valent-iron permeable reactive barriers-how long will they last? *Remediation* **2001**, *11*, 1–18.
88. Lee, G.; Rho, S.; Jahng, D. Design considerations for groundwater remediation using reduced metals. *Korean J. Chem. Eng.* **2004**, *21*, 621–628. [CrossRef]
89. Schreier, C.G.; Reinhard, M. Transformation of chlorinated organic compounds by iron and manganese powders in buffered water and in landfill leachate. *Chemosphere* **1994**, *29*, 1743–1753. [CrossRef]
90. Qiu, S.R.; Lai, H.-F.; Roberson, M.J.; Hunt, M.L.; Amrhein, C.; Giancarlo, L.C.; Flynn, G.W. Yarmoff Removal of contaminants from aqueous solution by reaction with iron surfaces. *Langmuir* **2000**, *16*, 2230–2236. [CrossRef]
91. Farrell, J.; Wang, J.; O'Day, P.; Conklin, M. Electrochemical and spectroscopic study of arsenate removal from water using zero-valent iron media. *Environ. Sci. Technol.* **2001**, *35*, 2026–2032. [CrossRef] [PubMed]
92. Mantha, R.; Taylor, K.E.; Biswas, N.; Bewtra, J.K. A continuous system for Fe^0 reduction of nitrobenzene in synthetic wastewater. *Environ. Sci. Technol.* **2001**, *35*, 3231–3236. [CrossRef] [PubMed]
93. Furukawa, Y.; Kim, J.-W.; Watkins, J.; Wilkin, R.T. Formation of ferrihydrite and associated iron corrosion products in permeable reactive barriers of zero-valent iron. *Environ. Sci. Technol.* **2002**, *36*, 5469–5475. [CrossRef] [PubMed]
94. Mielczarski, J.A.; Atenas, G.M.; Mielczarski, E. Role of iron surface oxidation layers in decomposition of azo-dye water pollutants in weak acidic solutions. *Appl. Catal. B* **2005**, *56*, 289–303. [CrossRef]
95. Jia, Y.; Aagaard, P.; Breedveld, G.D. Sorption of triazoles to soil and iron minerals. *Chemosphere* **2007**, *67*, 250–258. [CrossRef] [PubMed]
96. Gorski, C.A.; Scherer, M.M. Fe^{2+} sorption at the Fe oxide-water interface: A revised conceptual framework. In *Aquatic Redox Chemistry*; Tratnyek, P., Ed.; American Chemical Society: Washington, DC, USA, 2011; pp. 315–343.
97. Kamolpornwijit, W.; Liang, L. Investigation of gas production and entrapment in granular iron medium. *J. Contam. Hydrol.* **2006**, *82*, 338–356. [CrossRef] [PubMed]
98. Mayer, K.U.; Blowes, D.W.; Frind, E.O. Reactive transport modeling of an *in situ* reactive barrier for the treatment of hexavalent chromium and trichloroethylene in groundwater. *Water Resour. Res.* **2001**, *37*, 3091–3103. [CrossRef]
99. Li, L.; Benson, C.H.; Lawson, E.M. Modeling porosity reductions caused by mineral fouling in continuous-wall permeable reactive barriers. *J. Contam. Hydrol.* **2006**, *83*, 89–121. [CrossRef] [PubMed]
100. Jeen, S.W.; Mayer, K.U.; Gillham, R.W.; Blowes, D.W. Reactive transport modeling of trichloroethene treatment with declining reactivity of iron. *Environ. Sci. Technol.* **2007**, *41*, 1432–1438. [CrossRef] [PubMed]
101. Quarteroni, A. Mathematical models in science and engineering. *J. Notices AMS* **2009**, *56*, 1–13.
102. Noubactep, C. An analysis of the evolution of reactive species in Fe^0/H_2O systems. *J. Hazard. Mater.* **2009**, *168*, 1626–1631. [CrossRef] [PubMed]
103. Nkundimana, E.; Noubactep, C.; Uwamariya, V. Metallic iron for water treatment and environmental remediation: A handout to young researchers. *Fresenius Environ. Bull.* **2015**, *24*, 4842–4846.
104. Noubactep, C.; Licha, T.; Scott, T.B.; Fall, M.; Sauter, M. Exploring the influence of operational parameters on the reactivity of elemental iron materials. *J. Hazard. Mater.* **2009**, *172*, 943–951. [CrossRef] [PubMed]
105. Meinrath, G. Aquatic chemistry of uranium: A review focusing on aspects of environmental chemistry. *Freib. Online Geosci.* **1998**, *1*, 101–108.
106. Grauer, R. Solubility Limitations: An "Old Timer's" View. In *Modelling in aquatic Chemistry*; Grenthe, I., Puigdomenech, I., Eds.; OECD Publications: Pairs, France, 1997; pp. 131–152.
107. Johnson, T.L.; Scherer, M.M.; Tratnyek, P.G. Kinetics of halogenated organic compound degradation by iron metal. *Environ. Sci. Technol.* **1996**, *30*, 2634–2640.
108. Ebert, M.; Birke, V.; Burmeier, H.; Dahmke, A.; Hein, P.; Köber, R.; Schad, H.; Schäfer, D.; Steiof, M. Commentary on the contributions "The end of a myth" and "On the operating mode of reactive walls" by Dr. Chicgoua Noubactep. *Wasser Luft und Boden* **2007**, *7*, 4–5. (In German)

109. Elsner, M.; Cwiertny, D.M.; Roberts, A.L.; Lollar, B.S. Response to Comment on "1,1,2,2-Tetrachloroethane Reactions with OH^-, Cr(II), Granular Iron, and a Copper-Iron Bimetal: Insights from Product Formation and Associated Carbon Isotope Fractionation". *Environ. Sci. Technol.* **2007**, *41*, 7949–7950. [CrossRef]
110. Kang, S.-H.; Choi, W. Response to Comment on "Oxidative Degradation of Organic Compounds Using Zero-Valent Iron in the Presence of Natural Organic Matter Serving as an Electron Shuttle". *Environ. Sci. Technol.* **2009**, *43*, 3966–3967. [CrossRef]
111. Tratnyek, P.G.; Salter, A.J. Response to Comment on "Degradation of 1,2,3-Trichloropropane (TCP): Hydrolysis, Elimination, and Reduction by Iron and Zinc". *Environ. Sci. Technol.* **2010**, *44*, 3198–3199. [CrossRef]
112. Chen, L.; Jin, S.; Fallgren, P.H.; Liu, F.; Colberg, P.J.S. Passivation of zero-valent iron by denitrifying bacteria and the impact on trichloroethene reduction in groundwater. *Water Sci. Technol.* **2013**, *67*, 1254–1259. [CrossRef] [PubMed]
113. Hart, H. Critical reviews: The editor's point of view. *J. Chem. Doc.* **1968**, *8*, 241–244. [CrossRef]
114. Townsend, L.B. Critical reviews: The author's point of view. *J. Chem. Doc.* **1968**, *8*, 239–241. [CrossRef]
115. Berthod, A. So what? or required content of a review article. *Sep. Purif. Rev.* **2009**, *38*, 203–206. [CrossRef]
116. Lipczynska-Kochany, E.; Harms, S.; Milburn, R.; Sprah, G.; Nadarajah, N. Degradation of carbon tetrachloride in the presence of iron and sulphur containing compounds. *Chemosphere* **1994**, *29*, 1477–1489. [CrossRef]
117. Warren, K.D.; Arnold, R.G.; Bishop, T.L.; Lindholm, L.C.; Betterton, E.A. Kinetics and mechanism of reductive dehalogenation of carbon tetrachloride using zero-valence metals. *J. Hazard. Mater.* **1995**, *41*, 217–227. [CrossRef]
118. Lavine, B.K.; Auslander, G.; Ritter, J. Polarographic studies of zero valent iron as a reductant for remediation of nitroaromatics in the environment. *Microchem. J.* **2001**, *70*, 69–83. [CrossRef]
119. Gheju, M.; Balcu, I.; Vancea, C. An investigation of Cr(VI) removal with metallic iron in the co-presence of sand and/or MnO_2. *J. Environ. Manag.* **2016**, *170*, 145–151. [CrossRef] [PubMed]
120. Schneider, P.; Neitzel, P.L.; Osenbrück, K.; Noubactep, C.; Merkel, B.; Hurst, S. *In-situ* treatment of radioactive mine waters using reactive materials-results of field experiments in uranium ore mines in Germany. *Acta Hydrochem. Hydrobiol.* **2001**, *29*, 129–138. [CrossRef]
121. Noubactep, C. Aqueous contaminant removal by metallic iron: Is the paradigm shifting? *Water SA* **2011**, *37*, 419–426. [CrossRef]
122. Noubactep, C. Investigating the processes of contaminant removal in Fe^0/H_2O systems. *Korean J. Chem. Eng.* **2012**, *29*, 1050–1056. [CrossRef]
123. Noubactep, C. Metallic iron for safe drinking water worldwide. *Chem. Eng. J.* **2010**, *165*, 740–749. [CrossRef]
124. Noubactep, C.; Schöner, A. Metallic iron: dawn of a new era of drinking water treatment research? *Fresen. Environ. Bull.* **2010**, *19*, 1661–1668.
125. Noubactep, C. Metallic iron for safe drinking water production. *Freib. Online Geosci.* **2011**, *27*, 38–46.
126. Noubactep, C. Research on metallic iron for environmental remediation: stopping growing sloppy science. *Chemosphere* **2016**, *153*, 528–530. [CrossRef] [PubMed]